Kinetic Energy and Angular Distributions of He and Ar Atoms Evaporating from Liquid Dodecane

Enamul-Hasan Patel,[†] *Mark A. Williams,*[†] *Sven P. K. Koehler*[*†§‡]

[†] School of Chemistry, The University of Manchester, Manchester M13 9PL, UK

[§] Dalton Cumbrian Facility, The University of Manchester, Moor Row CA24 3HA, UK

[‡] Photon Science Institute, The University of Manchester, Manchester M13 9PL, UK

Abstract:

We report both kinetic energy and angular distributions for He and Ar atoms evaporating from $C_{12}H_{26}$. All result were obtained by performing molecular dynamics simulations of liquid $C_{12}H_{26}$ with around 10-20 noble gas atoms dissolved in the liquid, and by subsequently following the trajectories of the noble gas atoms after evaporation from the liquid. While He evaporates with a kinetic energy distribution of $(1.05\pm0.03) \times 2RT$ (corrected for the geometry used in experiments: $(1.08\pm0.03) \times 2RT$, experimentally obtained value: $(1.14\pm0.01) \times 2RT$), Ar displays a kinetic energy distribution that better matches a Maxwell-Boltzmann distribution at the temperature of the liquid $((0.99\pm0.04) \times 2RT)$. This behavior is also reflected in the angular distributions which are close to a cosine distribution for Ar, but slightly narrower - especially for faster atoms - in the case of He. This behavior of He is most likely due to the weak interaction potential between He and the liquid hydrocarbon.

Introduction

We have in a recent publication reported the kinetic energy distribution of He atoms evaporating

from liquid dodecane ($C_{12}H_{26}$) obtained by molecular dynamics simulations.[1] These

computational studies had been motivated by experimental work by Nathanson and co-workers

who had measured the kinetic energy distribution of He from liquid dodecane microjets under

vacuum using time-of-flight methods.[2] Both studies qualitatively agree that the He atom kinetic

energy distribution is non-Maxwellian with an average kinetic energy of $(1.14\pm0.01) \times 2RT$

(experimental, Ref. 2) and $(1.05\pm0.03) \times 2RT$ (theory, Ref. 1, but $(1.08\pm0.03) \times 2RT$ after

correction for the round cross-section of the molecular beam used in the experiments). Obtaining

these kinetic energy distributions experimentally is a major advance as it is generally very

challenging to measure any dynamics at liquid surfaces as their high vapor pressure makes

working under rarified vacuum conditions almost impossible. Evaporation is a thermally-induced

process, and hence one would in the first instance assume the kinetic energy distribution to

follow a Maxwell-Boltzmann distribution at the temperature of the liquid surface. The flux of

such speed distributions from a surface can be described by

$$P(v)\mathrm{d}v = \tfrac{1}{2} \left(\tfrac{m}{kT}\right)^2 v^3 \exp\left(-\tfrac{mv^2}{2kT}\right)\mathrm{d}v.$$

Eqn. 1

However, on a molecular level, one would imagine that those atoms or molecules at the liquid

surface that have a speed at the higher end of the Maxwell-Boltzmann distributions are the ones

that are more likely to evaporate, hence it is feasible that the speed distribution of evaporating

atoms or molecules is shifted to higher velocities. Another criterion other than just solely the

kinetic energy distribution is the angular distribution; it is well-known that pure thermal

processes typically follow a $\cos^n \theta$ angular distribution (where θ is the polar angle relative to the surface normal) where n equals 1, while superthermal processes often display a narrower distribution ($n > 1$).[3,4,5] We here present molecular dynamics simulations of both He and Ar evaporating from liquid dodecane, $C_{12}H_{26}$, in which we follow the trajectories of evaporating noble gas atoms which allows us to construct velocity distributions that can be analyzed both in terms of kinetic energy as well as angular distributions, and hence shed more light onto evaporation processes from liquid surfaces.

Details of the molecular dynamics simulations are essentially the same for both the He and Ar evaporation studies as far as the input is concerned, the only two differences being 1) the interaction potential between the atoms on the hydrocarbon chains and the He/Ar atoms (*e.g.* the well depth for He$\cdots$C interaction is 0.35 kJ mol^{-1} while it is 0.64 kJ mol^{-1} for Ar$\cdots$C interaction), and the mass of He *vs.* Ar, of course. (Since we add only 10-20 noble gas atoms into the liquid consisting of ~297 molecules/11286 atoms, we do not expect the He-He or Ar-Ar interaction to have an influence on the results.) The outcome from these studies provides a means to 'map' the interaction potentials between evaporating atoms and the liquid.

Experimentally, it is very challenging to measure velocity distributions of *nascent* atoms or molecules as such experiments have to be performed under vacuum in order for the nascent velocity distribution of the evaporating atoms/molecules *not* to be perturbed by collisions with background gas before they are detected. Early evaporation studies hence focused on sublimation to reduce vapor pressures; Klemperer observed thermal vibrational distributions of I_2 at the temperature of the solid iodine from which they were originating.[6] Padowitz and Sibener studied the sublimation of NO from solid NO films; they observed thermal rotational state distributions,

an angular flux that can be described by a cosine distribution, and drew conclusions regarding how these results would influence the molecular dynamics of NO molecules sticking to NO films.[7] Nesbitt and co-workers found that the rotational, vibrational, and translational energy distribution of CO_2 molecules subliming from thin CO_2 films can be described by a Boltzmann distribution characterized by the temperature of the thin film itself.[8] Early studies of actual liquids were initially concerned with slightly "esoteric" liquids such as liquid sodium, from which sodium dimers evaporate. The internal energy distribution of Na_2 was found to be thermal and can be described by the temperature of the liquid surface.[9,10] The use of a range of liquids with low vapor pressures (such as squalene, $C_{30}H_{62}$, or glycerin, $C_3H_8O_3$) for dynamics studies under vacuum conditions can mainly be attributed to the group of Nathanson.[11,12] They found that $e.g.$ HNO_3 evaporates from sulfuric acid solutions covered with a layer of hexanol with a Maxwell-Boltzmann distribution at the temperature of the liquid surface.[13]

Faubel's work in the late-80s lead to the development of liquid jets, which greatly increased the range of liquids whose interfacial dynamics could be studied under vacuum.[14,15] Faubel's group itself studied evaporation processes, in particular the evaporation of neat liquid jets; H_2O molecules evaporate from a room-temperature liquid water jet with a thermal kinetic energy distribution that can be described by a water temperature of ~210 K.[14] Dimers of e.g. acetic acid from neat liquids or their solution in water evaporate with a non-Maxwellian kinetic energy distribution that exceeds the liquid temperature by 100-200 K.[15] Buntine and co-workers measured a very fast rotational relaxation of benzene evaporating from water-ethanol mixtures, deducing that the rotational temperature mirrors the translational energy of the liquid jet, while vibrational relaxation is less efficient (but depends on the particular vibrational mode), and as such is more akin to the liquid surface temperature.[16,17] Saykally and co-workers even used

liquid jet experiments to detect isotope effects in the evaporation behavior of water.[18] Most relevant to the work presented here, Nathanson and his group have studied the evaporation of He from a range of hydrocarbons, and found kinetic energy distributions which in all cases exceeded the value expected for a thermal Maxwell-Boltzmann process of $2RT$.[19] Equally, He evaporation from water and salty solution result in super-Maxwellian speed distributions.[20] Conversely, evaporation of Ar from dodecane results in a velocity distribution that can be described by a Maxwell-Boltzmann distribution at the temperature of the liquid surface (private communications). Kann and Skinner thoroughly analyzed the dependence of kinetic energy and angular distribution of particles evaporating from liquid water on the well depth and the mass, essentially treating a generalized case for a range of masses/well depths, while this work is specifically treating He and Ar atoms only, with the main difference being the solvent (dodecane *vs.* water) used. Broadly speaking, they find that heavier atoms which are weakly interacting with the solvent result in super-Maxwellian kinetic energy distributions of the evaporating atoms, while light atoms strongly interacting (deep well depth, high ϵ in the Lennard-Jones potential) with the solvent yield sub-Maxwellian behavior.[21]

In analyzing the above results collectively, it appears as if atoms or molecules from a pure liquid predominantly evaporate with internal and translational energy distributions that can be described by a Maxwell-Boltzmann distribution at the temperature of the liquid surface, whereas solutions typically deviate from this behavior. One point worth noting is that the experiments employing liquid jets under vacuum observe processes which are *not* in equilibrium, i.e. evaporation is a one-sided process not counter-acted by condensation. While this limitation differentiates the experiments from the "real world", it has the advantage, however, that the evaporation process can be studied in isolation. As for the simulations, the vacuum space above

the liquid slab in our simulations is too small to even accommodate one gas-phase dodecane molecule at a vapor pressure of 18 Pa; however, He atoms – once evaporated from the liquid – do reach the opposite liquid interface again after a flight path of around 90 Å, but their velocity 20 Å from the opposite liquid surface is not counted, and their flux so low that they do not influence the evaporation process.

Simulations of evaporation from model liquids into vacuum have been performed for generalized cases,[22,23] and even internal energy distributions predicted.[24,25] Somasundaram and Lynden-Bell predicted thermal velocity distributions for CO_2 and N_2 evaporating from water by MD simulations,[26] and Varilly and Chandler find a Maxwellian energy distribution of evaporating water using sophisticated studies employing the SPC/E molecular mechanics model for water.[27]

We have chosen the system of He and Ar in dodecane, $C_{12}H_{26}$, because a) dodecane is a common solvent and the major constituent of kerosene, important in many technological applications, and b) because results can be directly compared to the recent results by Nathanson and co-workers. The major difference between the noble gases He and Ar is – apart from their mass – their different polarizability, with He being the least-polarizable element in the period table; Ar hence has a deeper well due to dispersion forces. The work presented here hence seeks to gain a molecular level understanding of evaporation of two different noble gases from liquid hydrocarbons using MD simulations; this is not only of fundamental importance as it advances our understanding of physico-chemical processes at liquid interfaces, but is also relevant to a range of practical applications, be they processes at the surface of the sea, atmospheric processes (on e.g. aerosol particles), and technological processes at liquid interfaces (e.g. solvent extraction). This work not only computes the kinetic energy distribution of evaporating noble gas

atoms, but adds the angular distribution, which is notoriously difficult to obtain using (round) liquid jet experiments.

Methods

We employed the all-atom 1995 release of the AMBER force field (Ref. 28) as done in our previous work (Ref. 1) for the molecular dynamics simulations of dodecane. As a general purpose force field, AMBER has successfully been used for modelling liquids, and also well reproduced the bulk density of our liquid when compared to other force fields. However, since AMBER does not include parameters for non-bonded interactions with neutral He atoms, these values were taken from the United Force Field (UFF).[29] The non-bonding interaction between atoms of different dodecane molecules, atoms in the same molecule separated by more than three bonds (i.e. whose interaction is not governed by bond distance, angular, or torsional potentials), or between helium atoms and atoms in dodecane molecules is described by Lennard-Jones 12-6 potentials. Lorentz-Berthelot combining rules were applied for interactions between unlike atoms. The cutoff for the interatomic forces was chosen to be 12 Å.

Bond lengths as well as bond angles are described by harmonic potentials, while the torsional potential is described by a cosine potential. The simulations were implemented in DL_POLY 4.03 and were run in an *NVT* ensemble at a temperature of 298 K regulated by a Nosé–Hoover thermostat.[30] The molecular dynamics simulations were run with a timestep of 1 fs. The relaxed dodecane slab (density = 746.0 g L^{-1})[31] was located in the center of our simulation box ($53.60 \times 46.34 \times 136.48$ Å^3), occupying one third of the volume. Periodic boundary conditions (PBC) were applied in all three dimensions.

We randomly selected almost 1000 different relaxed dodecane configurations and inserted He or Ar atoms in the liquid with the following constraints: 1) He/Ar atoms must be at least 2 Å away from any surrounding atoms. 2) Every two noble gas atoms must be at least 12 Å apart. 3) He/Ar atoms must be at least 4 Å below the Gibbs dividing surface. This resulted in roughly between 10 and 20 noble gas atoms in each liquid slab, and the atoms were given a kinetic energy corresponding to a 298 K Boltzmann distribution. Once the configurational energy had stabilized and equilibration was reached again, we monitored the position of the He or Ar atoms. Whenever a He/Ar atom passed through an imaginary plane parallel to and 20 Å above the liquid interfaces, its velocity was recorded and the atom not considered further (*i.e.* it was ignored even if it re-entered the detection region due to the PBCs), see Fig. 1. This procedure was continued until around 75% of either He or Ar atoms had evaporated. We thus accumulated the velocities of >9,000 He atoms and close to 2000 Ar atoms, and these velocities were binned in 20 m s^{-1} wide intervals.
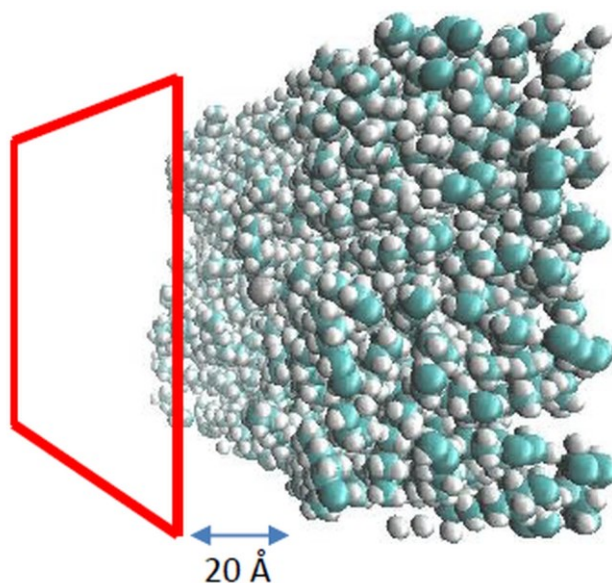

20 Å

Figure 1. Illustration of a relaxed dodecane slab (C atoms: turquoise; H atoms: white) with an imaginary plane 20 Å above the liquid-vacuum interface where the traversing He or Ar atoms are counted.

Results and Discussion

The binned velocity distributions for He and Ar were fitted to eqn. 1. We note that these velocity distributions do not necessarily need to follow a Maxwell-Boltzmann distribution, but 1) the resulting single temperature from the fit is a good initial indication for any deviation from the liquid temperature, and 2) the distributions appear to not deviate too much from a Maxwell-Boltzmann distribution. These flux distributions are subsequently converted to energy distributions, see Fig. 2, and the average kinetic energy is extracted from the fits. We had previously reported a value of $(1.05\pm0.03) \times 2RT$ for the average kinetic energy distribution of He atoms evaporating from the flat (i.e. no curvature) dodecane surface in our simulations; if corrected for the curved surface of the liquid jet experiments by a factor of $1/\sin \theta$, where θ is the polar angle, this average kinetic energy becomes $(1.08\pm0.03) \times 2RT$. The average kinetic energy of Ar after application of the correct Jacobian to the velocity distribution is $(0.99\pm0.04) \times 2RT$; this equates to $(1.02\pm0.04) \times 2RT$ for the purpose of comparison with the liquid jet experiments. In the experimental work from a round liquid jet, average kinetic energy distributions of $(1.14\pm0.01) \times 2RT$ for He evaporation and close to $2RT$ for Ar evaporation were measured, but since angular information cannot be extracted until experiments are repeated with flat liquid jets, we performed the above conversion of our results for comparison.
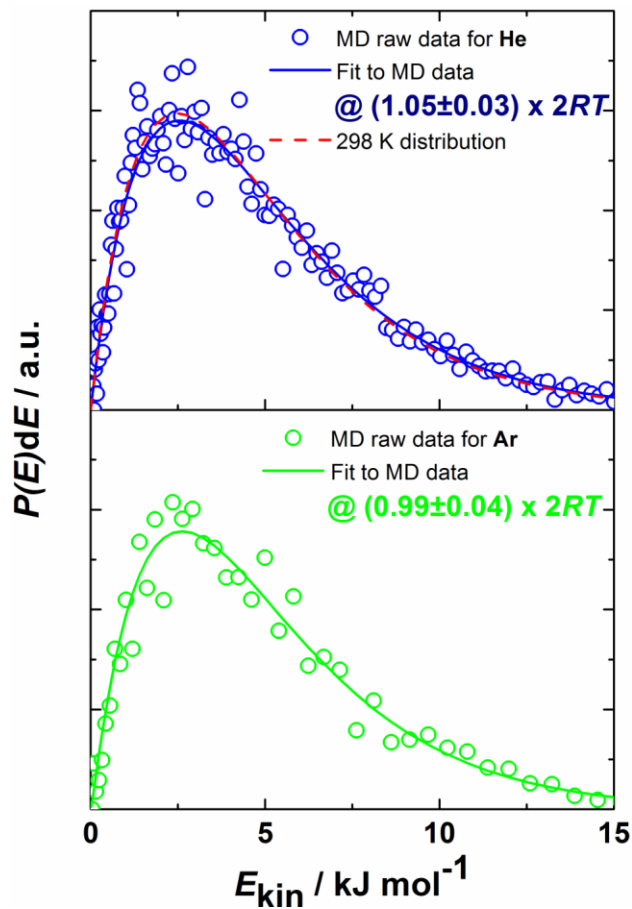
Figure 2. Flux distributions $P(E)dE$ of He (top) and Ar (bottom) atoms evaporating from dodecane as a function of their kinetic energy. Circles are raw data from MD simulations, straight lines are best fits to equation 1, and the errors are standard deviations from the fits. Red dashed line in top panel is a 298 K distribution, which is omitted in the bottom panel as it overlaps with the best fit in green.

Since we recorded the three velocity components v_x, v_y, and v_z separately for each evaporating He or Ar atom, we could also extract angular information in the form of the polar angle, i.e. the angle between the outgoing noble gas atom and the surface normal. The Maxwell-Boltzmann flux distribution taking angular orientation into account is given by eqn. 2

$$P_{\text{MB}}(v, \theta) \sin\theta \; d\theta \; dv = 2\pi c \left(\frac{m}{2\pi kT}\right)^{3/2} \exp\left(\frac{-mv^2}{2kT}\right) v^3 \cos\theta \; \sin\theta \; d\theta \; dv$$

<div align="right">Eqn. 2</div>

which results in a cos θ angular distribution.[26] Fig. 3 shows the polar angle for the He atoms and Ar atoms averaged over *all* velocities.
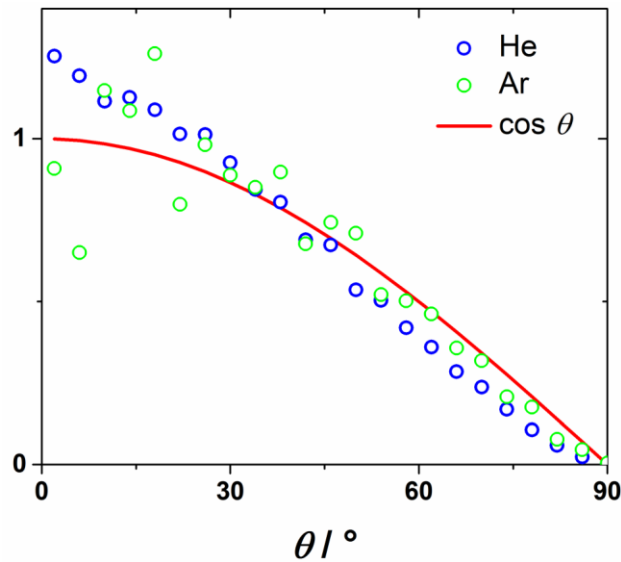

Figure 3. Normalized distribution of polar angles θ of He (blue circles) and Ar (green circles) evaporating from dodecane compared to a cos θ distribution (red line).

Both distributions follow the cos θ distribution passably, but deviate to lower intensities at polar angles close to 90°, and show higher intensity along the surface normal, which is more pronounced in the case of He. One reason for the larger scatter in the Ar data is simply the smaller number of trajectories analyzed. It also appears as if the He angular distribution is slightly narrower than the Ar distribution. This is in agreement with the work by Kann and

Skinner who find that atoms interacting weakly with the solvent (low ϵ) result in an angular distribution more aligned along the surface normal.[21]

In order to correlate the angular distribution to the kinetic energy, we analysed the angular distributions for He and Ar atoms leaving the surface with an energy between 0 and 5 kJ mol^{-1}, 5 to 10 kJ mol^{-1}, and 10 to 15 kJ mol^{-1} separately, thus capturing almost all evaporating atoms, see Fig. 2. These distributions are shown in Fig. 4.
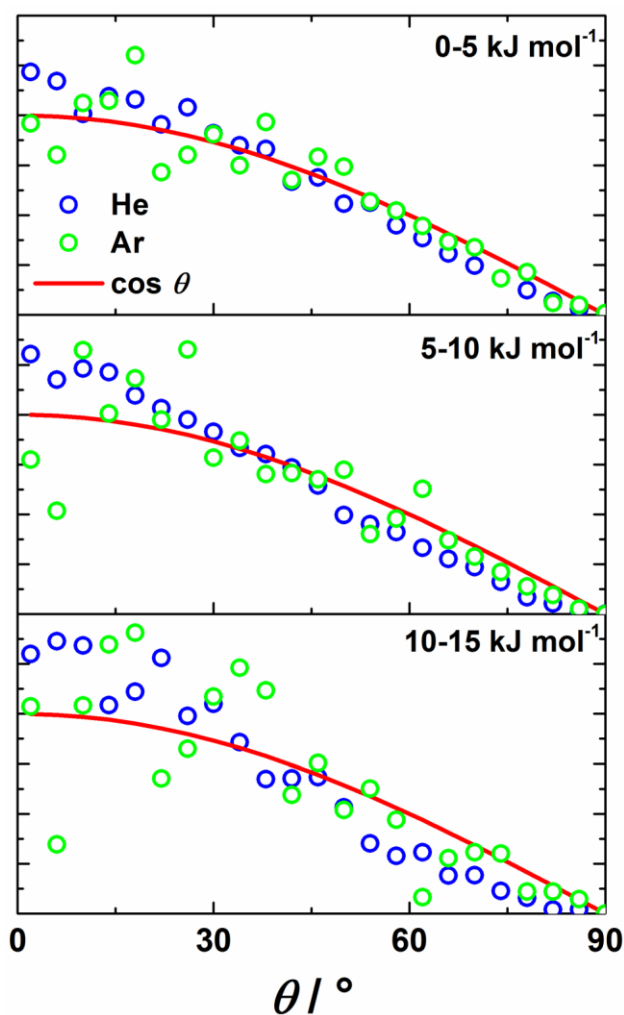
Figure 4. Distributions of polar angles for He (blue circles) and Ar (green circles) separated according to their kinetic energy. The red curve in each graph is a $\cos \theta$ distribution for comparison.

It can be seen that the angular distributions follow a cosine distribution better for kinetic energies between 0 and 5 kJ mol^{-1}, but for the highest kinetic energies (10 to 15 kJ mol^{-1}), the simulations result in a lower intensity at polar angles close to 90°, but a higher intensity along the surface normal, at least for He. Non-thermal desorption processes that do not follow a Maxwell-Boltzmann distribution but are nonetheless symmetric around the surface normal can often be fitted to a $\cos^n \theta$ distribution;[4,5] any deviation in n from 1 indicates non-thermal behavior, and an increase in n not only indicates a narrower distribution, but also a greater deviation from thermal behavior. In order to quantify the above observation further, we have fitted the data in Fig. 4 to $\cos^n \theta$ distributions, these fitting parameters are shown in Table 1.

Table 1. Fitting parameters (to a $\cos^n \theta$ function) of the angular distributions of He and Ar evaporation for different kinetic energies; errors are standard deviations. N_{atom} are the absolute number of atoms used for the analysis of each bin.

	n_{He}	N_{He}	n_{Ar}	N_{Ar}
0 kJ mol^{-1} < E_{kin} ≤ 5 kJ mol^{-1}	1.18±0.08	5322	1.02±0.09	1084
5 kJ mol^{-1} < E_{kin} ≤ 10 kJ mol^{-1}	1.30±0.14	2797	1.05±0.16	667
10 kJ mol^{-1} < E_{kin}	1.42±0.19	940	1.10±0.22	247
Σ atoms		9059		1998

θ is the polar angle between the noble gas atom trajectory and the surface normal.

Two observations are noteworthy: 1) The fitting parameter n increases for both He and Ar as the kinetic energy increases, *i.e.* faster atoms have a tendency to evaporate within a narrower cone along the surface normal. 2) The He angular distribution is narrower in all cases as compared to the Ar distribution, in fact even the slowest He atoms have a narrower angular distribution than the fastest Ar atoms. This second point is not unexpected as the He kinetic energy distribution already displayed a deviation from thermal behavior, and this is reinforced by its angular distribution. One would also intuitively expect the faster atoms to evaporate with a narrower angular distribution; it is interesting to note, though, that the increase in n is greater for He than for Ar when moving to the highest kinetic energies (He: $1.18 \rightarrow 1.42 \cong 20\%$; Ar: $1.02 \rightarrow 1.10 \cong$ 8%). As discussed previously, we believe that the shift to higher kinetic energies for He is due to the cone mechanism; in the cone mechanism, a He atom finds itself in a cone-shaped opening/crater within the liquid surface but below the Gibbs dividing surface. Since it is repelled by the surrounding alkyl chains, it is accelerated to the opening of the cone and expelled from the liquid with a higher kinetic energy, and preferentially along the surface normal.[1] This only occurs to a small fraction of the He atoms, and could in principle happen to any evaporating particle. However, Ar is more strongly attracted to the alkyl chains, and is hence less likely to be expelled from such a cone. The kinetic energy distribution of Ar can indeed be described by a Maxwell-Boltzmann distribution at the surface temperature, and it lacks these directed higher-energy atoms. One can in fact argue that the angular distribution of Ar atoms follows a standard $\cos \theta$ distribution (*i.e.* with $n \sim 1$), at least for those atoms with energies between 0 and 10 kJ mol^{-1} (and similar to the findings by Kann and Skinner[21]), and hence does not deviate much from a thermal Maxwell-Boltzmann distribution in either its energy nor angular distribution.

In support of the above, we have investigated the contribution to the average kinetic energy distribution ($2RT$ for a Maxwell-Boltzmann distribution) of the parallel and perpendicular (to the surface) flux of atoms. For He, the 2D speed distribution parallel to the liquid surface contributes slightly less than RT to the overall kinetic energy ($0.98 \times 2RT$), while the contribution along the surface normal more than compensates for that to yield $<E_{kin}> = 1.05 \times 2RT$; this is in close agreement with the work by Kann and Skinner who find that the tangential component of the kinetic energy distribution (*i.e.* parallel to the surface) never exceeds RT for their parameter range studied.[21] However, for Ar, neither the average energy of the perpendicular nor of the parallel component deviate much from RT for lower overall kinetic energies in this work, with the perpendicular component only becoming dominant at the highest energies. Similarly, Kann and Skinner only find a slight preference for evaporation along the surface normal for the Ar/H_2O case.[21] Even though the solvent (water) in the work by Kann and Skinner is more polarizable, leading to stronger interaction with the evaporating atoms (higher ϵ values overall), it seems that the trends observed by Kann and Skinner, namely the angular distribution of evaporating atoms being aligned along the surface normal for weakly interacting particles, and the small deviations from a Maxwellian distribution for the tangential component, also apply to the He/$C_{12}H_{26}$ and the Ar/$C_{12}H_{26}$ cases studied here.

The results for the kinetic energy distribution – and to a lesser extent the angular distribution – carry some significance if one was interested in the reverse process, *i.e.* the adsorption or in fact absorption of noble gas atoms onto and into liquids. Based on the principle of microscopic reversibility, detailed balance dictates that every step at a molecular level must be reversible with the same energy distribution as the initial step.[4] That means for these evaporation studies that the kinetic energy distributions provide a clue as to which He and Ar atoms would adsorb onto or

absorb into the liquid dodecane surface. Since the kinetic energy distribution of He evaporating from a liquid dodecane surface is shifted to higher energies compared to a thermal Maxwell-Boltzmann distribution, one can hence conclude that the kinetic energy distribution of He atoms impinging on *and* adsorbing to the liquid surface must also be shifted to slightly higher energies. The distribution of Ar atoms impinging at the surface and being adsorbed would follow a Maxwell-Boltzmann kinetic energy distribution, though. The rationale behind this is that the interatomic forces between He and the hydrocarbon chains are weaker than for Ar, *i.e.* the potential well-depth is shallower; a He atom impinging with a low velocity may not be captured and bounce off the surface because the attractive potential is so shallow, whereas a fast He atom may impinge on the surface in a reverse process to the cone mechanism, *i.e.* it may follow a trajectory to the bottom of a cone/crater that temporarily opens up, or even drill itself into the liquid due to its high kinetic energy. For Ar, however, the attractive potential encountered even by slower atoms when approaching the surface is strong enough for them to be adsorbed, and hence the kinetic energy distribution of those Ar atoms that adsorb onto and absorb into the liquid resembles a thermal Maxwell-Boltzmann distribution. This is highlighted in Fig. 5 which shows the ratio of the calculated kinetic energy distribution of the desorbing noble gas atoms and a Maxwell-Boltzmann distribution at the temperature of the liquid. Any deviation from a thermal MB behavior is recognized by a deviation from the horizontal line through $y = 1$. It can be seen that this line is above 1 for higher energies of He, but below 1 (but to a lesser degree) for Ar. The sharp increase as one approaches zero kinetic energy is mainly due to the steep slope of the MB distribution close to zero, such that any deviation from a MB behavior in that region results in large ratios.
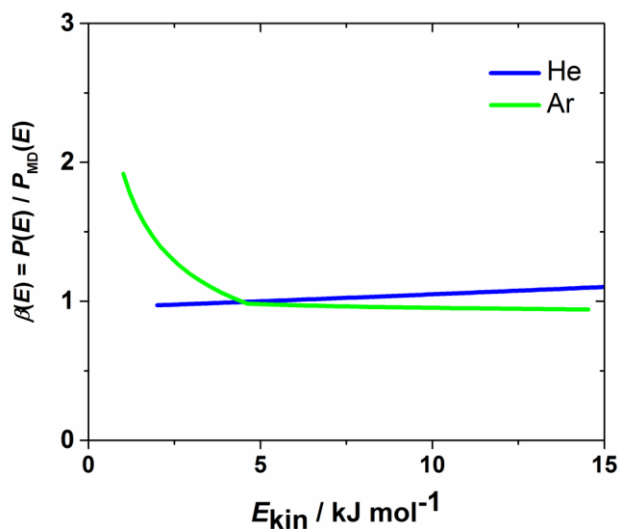
Figure 5. Ratio of probability flux distribution for He and Ar evaporating from liquid dodecane and a 298 K Maxwell-Boltzmann distribution.

Conclusions

The molecular dynamics simulations presented here were performed to model the kinetic energy distribution of the noble gas atoms He and Ar as they evaporate from liquid dodecane, $C_{12}H_{26}$, and to compare these results to experimental data obtained by Nathanson's group by using a combination of liquid jet and time-of-flight methods. The simulations and experiments at least qualitatively agree that He seems to evaporate with a slightly higher kinetic energy distribution compared to a MB distribution at the temperature of the liquid surface, whereas Ar closely follows a MB distribution. The angular distributions behave similarly, i.e. they can satisfactorily be described by a $\cos^n \theta$ distribution for Ar with n barely deviating from 1, whereas n is larger for He, indicating that it evaporates with a narrower distribution along the surface normal. This has implications for the adsorption behavior, since He is now expected to preferentially adsorb when it impinges with a higher kinetic energy on average as compared to a thermal MB distribution for Ar.

AUTHOR INFORMATION

Corresponding Author

* Email: sven.koehler@manchester.ac.uk

The University of Manchester

School of Chemistry

Manchester

M13 9PL, UK

+44 161 306 4448

Reference list:

[1] Williams, M. A.; Koehler, S. P. K. MD Simulations of He Evaporating from Dodecane. *Chem. Phys. Lett.* **2015**, *629*, 53-57.

[2] Johnson, A. M.; Lancaster, D. K.; Faust, J. A.; Hahn, C.; Reznickova, A.; Nathanson, G. M. Ballistic Evaporation and Solvation of Helium Atoms at the Surfaces of Protic and Hydrocarbon Liquids. *J. Phys. Chem. Lett.* **2014**, *5*, 3914-3918.

[3] Comsa, G. Angular Distribution of Scattered and Desorbed Atoms from Specular Surfaces. *J. Chem. Phys.* **1967**, *48*, 3235-3240.

[4] Comsa, G.; David, R. Dynamical Parameters of Desorbing Molecules. *Surf. Sci. Rep.* **1985**, *5*, 145-198.

[5] Rettner, C. T.; Auerbach, D. J. Distinguishing the Direct and Indirect Products of a Gas-Surface Reaction. *Science* **1994**, *263*, 365-367.

[6] Brown, R.L.; Brewer, R.G.; Klemperer, W. Vibrational Distribution in Evaporating Iodine. *J. Chem. Phys.* **1962**, *36*, 1827-1831.

[7] Padowitz, D.F.; Sibener, S.J. Sublimation of Nitric Oxide Films: Rotational and Angular Distributions of Desorbing Molecules. *Surf. Sci.* **1989**, *217*, 233-246.

[8] Weida, M. J.; Sperhac, J. M.; Nesbitt, D. J. Sublimation Dynamics of CO_2 Thin Films: A High Resolution Diode Laser Study of Quantum State Resolved Sticking Coefficients. *J. Chem. Phys.* **1996**, *105*, 749-766.

[9] Miksch, G.; Weber, H. G. Laser Diagnostics of Surface-Emitted Na_2 Molecules. *Chem. Phys. Lett.* **1982**, *87*, 544-547.

[10] Becker, C. H. Laser and Ion Beam Studies of Liquid Sodium Surface Chemistry and Na_2 Evaporation. *Surf. Sci.* **1985**, *149*, 67-80.

[11] Nathanson, G. M. Molecular Beam Studies of Gas-Liquid Interfaces. *Annu. Rev. Phys. Chem.* **2004**, *55*, 231-255.

[12] Saecker, M. E.; Nathanson, G. M. Collisions of Protic and Aprotic Gases with Hydrogen Bonding and Hydrocarbon Liquids. *J. Chem. Phys.* **1993**, *99*, 7056-7075.

[13] Park, S.-C.; Burden, D. K.; Nathanson, G. M. The Inhibition of N2O5 Hydrolysis in Sulfuric Acid by 1-butanol and 1-hexanol Surfactant Coatings. *J. Phys. Chem. A* **2007**, *111*, 2921-2929.

[14] Faubel, M.; Schlemmer, S.; Toennies, J. P. A Molecular Beam Study of the Evaporation of Water from a Liquid Jet. *Z. Phys. D* **1988**, *10*, 269-277.

[15] Faubel, M.; Kisters, T. Non-equilibrium Molecular Evaporation of Carboxylic Acid Dimers. *Nature* **1989**, *339*, 527-529.

[16] Maselli, O. J.; Gascooke, J. R.; Lawrance, W. D.; Buntine, M. A. Benzene Internal Energy Distributions Following Spontaneous Evaporation from a Water-Ethanol Solution. *J. Phys. Chem. C* **2009**, *113*, 637-643.

[17] Maselli, O. J.; Gascooke, J. R.; Lawrance, W. D.; Buntine, M. A. The Dynamics of Evaporation from a Liquid Surface. *Chem. Phys. Lett.* **2011**, *513*, 1-11.

[18] Cappa, C. D.; Drisdell, W. S.; Smith, J. D.; Saykally, R. J.; Cohen, R. C. Isotope Fractionation of Water during Evaporation without Condensation. *J. Phys. Chem. B* **2005**, *109*, 24391-24400.

[19] Lancaster, D. K.; Johnson, A. M.; Kappes, K.; Nathanson, G. M. Probing Gas-Liquid Interfacial Dynamics by Helium Evaporation from Hydrocarbon Liquids and Jet Fuels. *J. Phys. Chem. C* **2015**, *119*, 14613-14623.

[20] Hahn, C.; Kann, Z. R.; Faust, J. A.; Skinner, J. L.; Nathanson, G. M. Super-Maxwellian Helium Evaporation from Pure and Salty Water. *J. Chem. Phys.* **2016**, *144*, 044707.

[21] Kann, Z. R.; Skinner, J. L. Sub- and Super-Maxwellian Evaporation of Simple Gases from Liquid Water. *J. Chem. Phys.* **2016**, *144*, 154701.

[22] Frezzotti, A.; Gibelli, L.; Lorenzani, S. Mean Field Kinetic Theory Description of Evaporation of a Fluid into Vacuum. *Phys. Fluids* **2005**, *17*, 012102.

[23] Matsumoto, M. Molecular Dynamics of Fluid Phase Change. *Fluid Phase Equilib.* **1998**, *144*, 307-314.

[24] Ishiyama, T.; Yano, T.; Fujikawa, S. Molecular Dynamics Study of Kinetic Boundary Condition at an Interface between a Polyatomic Vapor and its Condensed Phase. *Phys. Fluids* **2004**, *16*, 4713-4726.

[25] Frezzotti, A. A Numerical Investigation of the Steady Evaporation of a Polyatomic Gas. *Eur. J. Mech. B: Fluids* **2007**, *26*, 93-104.

[26] Somasundaram, T.; Lynden-Bell, R. M. The Velocity Distribution of Desorbing Molecules: a Simulation Study. *Mol. Phys.* **1999**, *97*, 1029-1034.

[27] Varilly, P.; Chandler, D. Water Evaporation: A Transition Path Sampling Study. *J. Phys. Chem. B* **2013**, *117*, 1419-1428.

[28] Cornell, W. D.; Cieplak, P.; Bayly, C. I.; Gould, I. R.; Merz, K. M.; Ferguson, D. M.; Spellmeyer, D. C.; Fox, T.; Caldwell, J. W.; Kollman, P. A. A Second Generation Force Field for

the Simulation of Proteins, Nucleic Acids, and Organic Molecules. *J. Am. Chem. Soc.* **1995**, *117*, 5179-5197.

[29] Rappe, A. K.; Casewit, C. J.; Colwell, K. S.; Goddard III, W. A.; Skiff, W. M. UFF, a Full Periodic Table Force Field for Molecular Mechanics and Molecular Dynamics Simulations. *J. Am. Chem. Soc.* **1992**, *114*, 10024-10035.

[30] Todorov, I. T.; Smith, W.; Trachenko, K.; Dove, M. T. DL_POLY_3: New Dimensions in Molecular Dynamics Simulations via Massive Parallelism. *J. Mater. Chem.* **2006**, *16*, 1911-1918.

[31] Caudwell, D. R.; Trusler, J. P. M.; Vesovic, V.; Wakeha, W. A. The Viscosity and Density of n-Dodecane and n-Octadecane at Pressures up to 200 MPa and Temperatures up to 473 K. *Int. J. Thermophys.* **2004**, *25*, 1339-1352.

TOC Graphic: